Original Article

Development and validation of a nomogram for predicting the need for concomitant endoscopic septoplasty during endonasal endoscopic dacryocystorhinostomy

Kerui Wang[1#], Xinyue Yu[1#], Rongxin Chen[1], Lixu Guo[1], Jing Li[1], Ziwei Meng[1], Yu Hu[2], Shihuai Nie[1], Xuanwei Liang[1^]

[1]State Key Laboratory of Ophthalmology, Zhongshan Ophthalmic Center, Sun Yat-sen University, Guangzhou, China; [2]Ophthalmologic Center, The First People's Hospital of Kashi Prefecture, The Affiliated Kashi Hospital of Sun Yat-Sen University, Kashi, China

Contributions: (I) Conception and design: K Wang, X Yu, X Liang; (II) Administrative support: X Liang, R Chen, S Nie; (III) Provision of study materials or patients: L Guo, S Nie, X Liang; (IV) Collection and assembly of data: K Wang, J Li, Z Meng, Y Hu; (V) Data analysis and interpretation: K Wang, X Yu; (VI) Manuscript writing: All authors; (VII) Final approval of manuscript: All authors.

[#]These authors contributed equally to this work as co-first authors.

Correspondence to: Shihuai Nie, BD; Xuanwei Liang, MD, PhD. State Key Laboratory of Ophthalmology, Zhongshan Ophthalmic Center, Sun Yat-sen University, 54 South Xianlie Road, Guangzhou 510060, China. Email: nieshh@mail.sysu.edu.cn; liangxuanwei@163.com.

Background: Simultaneous endoscopic septoplasty is often required during endonasal endoscopic dacryocystorhinostomy (En-DCR) to improve access to the lacrimal sac and potentially optimize surgical success rates. In current practice, the decision to proceed to concomitant endoscopic septoplasty during En-DCR in patients with primary acquired nasolacrimal duct obstruction (PANDO) is determined by anterior rhinoscopy and nasal endoscopic examination. However, none of these methods can be used to quantitatively assess the severity of septal deviation to determine the need for concomitant endoscopic septoplasty during En-DCR. This study was thus conducted to develop and validate a radiological prediction model based on computed tomography (CT) to predict the necessity of concomitant endoscopic septoplasty during En-DCR.

Methods: Data from 225 patients with PANDO and nasal septal deviation (NSD) who had undergone unilateral En-DCR in a single center from January 2022 to June 2023 were retrospectively analyzed. Least absolute shrinkage and selection operator (LASSO) was used to select predictors for concomitant endoscopic septoplasty during En-DCR. The ultimate model was developed through the application of multivariable logistic regression and subsequently confirmed through assessment with an internal validation cohort. The final model was then visually represented using a nomogram and an online calculator.

Results: In this retrospective study of 225 eyes from 225 patients with PANDO and NSD, the training cohort included 157 eyes, and the validation cohort included 68 eyes. CT imaging characteristics including NSD angle [odds ratio (OR) 1.54; 95% confidence interval (CI): 1.32–1.87], NSD location (OR 4.49; 95% CI: 1.25–18.77), NSD direction (OR 5.38; 95% CI: 1.48–24.52), and middle nasal passage width (MNPW) at the surgical side (OR 0.61; 95% CI: 0.43–0.82) were identified as independent predictors for concomitant endoscopic septoplasty during En-DCR. A novel nomogram constructed from these CT signs showed high predictive performance. The area under the curves (AUCs) of the training set and internal validation set were 0.913 and 0.909, respectively.

^ ORCID: 0000-0001-5408-5538.

Conclusions: A CT-based radiological prediction model was created to help surgeons determine if concomitant endoscopic septoplasty is needed during En-DCR in patients with PANDO and NSD.

Keywords: Endonasal endoscopic dacryocystorhinostomy (En-DCR); nasal septum deviation; computed tomography (CT); nomogram

Submitted Apr 09, 2024. Accepted for publication Jul 08, 2024. Published online Aug 05, 2024.
doi: 10.21037/qims-24-726
View this article at: https://dx.doi.org/10.21037/qims-24-726

Introduction

Primary acquired nasolacrimal duct obstruction (PANDO) secondary to chronic dacryocystitis (CD) is a common eye infection disorder (1,2). Endonasal endoscopic dacryocystorhinostomy (En-DCR), a minimally invasive procedure, has recently become a popular surgical approach for addressing nasolacrimal duct obstruction since it does not cause face scarring or harm the medial canthal ligament (3-5). However, surgical failure rates reported in the literature vary from 4% to 13%, with factors such as nasal septal deviation (NSD), concha bullosa, and nasal polyposis believed to impede surgical access and impact outcomes (6,7).

NSD is present to varying degrees in a significant proportion of the population (8). A concomitant NSD to the side of the nasal lacrimal ductal obstruction (NLDO) can obscure the insertion of the middle nasal turbinate into the lateral wall of the nose and prevent exposure of the lacrimal sacs, which may cause the failure of En-DCR (6,9,10). Therefore, a simultaneous endoscopic septoplasty is commonly performed to improve access to the lacrimal sac and potentially increase surgical success rates. Previous reports suggest that concomitant endoscopic septoplasty during En-DCR does not affect surgical prognosis but does reduce complications and that septoplasty should be considered when indicated to improve surgical access (11,12).

In current practice, the decision to proceed to concomitant endoscopic septoplasty during En-DCR in patients with PANDO is determined by anterior rhinoscopy and nasal endoscopic examination (13-15). In cases of mild NSD, topical nasal decongestion and vasoconstriction are typically effective in providing adequate surgical exposure. In instances of moderate-to-severe NSD, nasal septoplasty may be necessary during the same operative session to optimize surgical visualization. Both anterior rhinoscopy and nasal endoscopic examination are subjective methods used to determine the severity of NSD that can be affected by the experience of surgeon and the use of topical nasal decongestion and vasoconstriction. Computed tomography (CT) is helpful for evaluating structures near the nasolacrimal drainage system. When combined with dacryocystography (DCG), CT can clearly show the relationship between the drainage system and surrounding tissues and bones (16,17). However, some studies have suggested that CT should not be used to evaluate septal deviation since its findings differ from those of physical examination and are not associated with the Nasal Obstruction Symptom Evaluation score (13,18-21). In patients with PANDO and asymptomatic NSD, concomitant septoplasty is performed with the aim of creating a wide surgical corridor for En-DCR rather than relieving nasal obstruction symptoms. Therefore, CT scans may provide useful information to guide the surgical decision for septoplasty in these patients with PANDO.

Therefore, this study reviewed the imaging data of patients with PANDO to construct and validate a nomogram to predict the need for combined septal deviation correction during En-DCR. We present this article in accordance with the TRIPOD reporting checklist (available at https://qims.amegroups.com/article/view/10.21037/qims-24-726/rc).

Methods

Study design and populations

This retrospective study included data from patients with PANDO who selected surgical treatment for consecutive epiphora or mucopurulent discharge. This study was conducted in accordance with the Declaration of Helsinki (as revised in 2013) and was approved by the Institutional Review Board of Zhongshan Ophthalmic Center of Sun Yat-Sen University (No. 2021KYPJ100). The requirement for written informed consent was waived due to the retrospective nature of the analysis. From January 2022 to June 2023, data from consecutive patients diagnosed with PADNO who had undergone surgery at Zhongshan

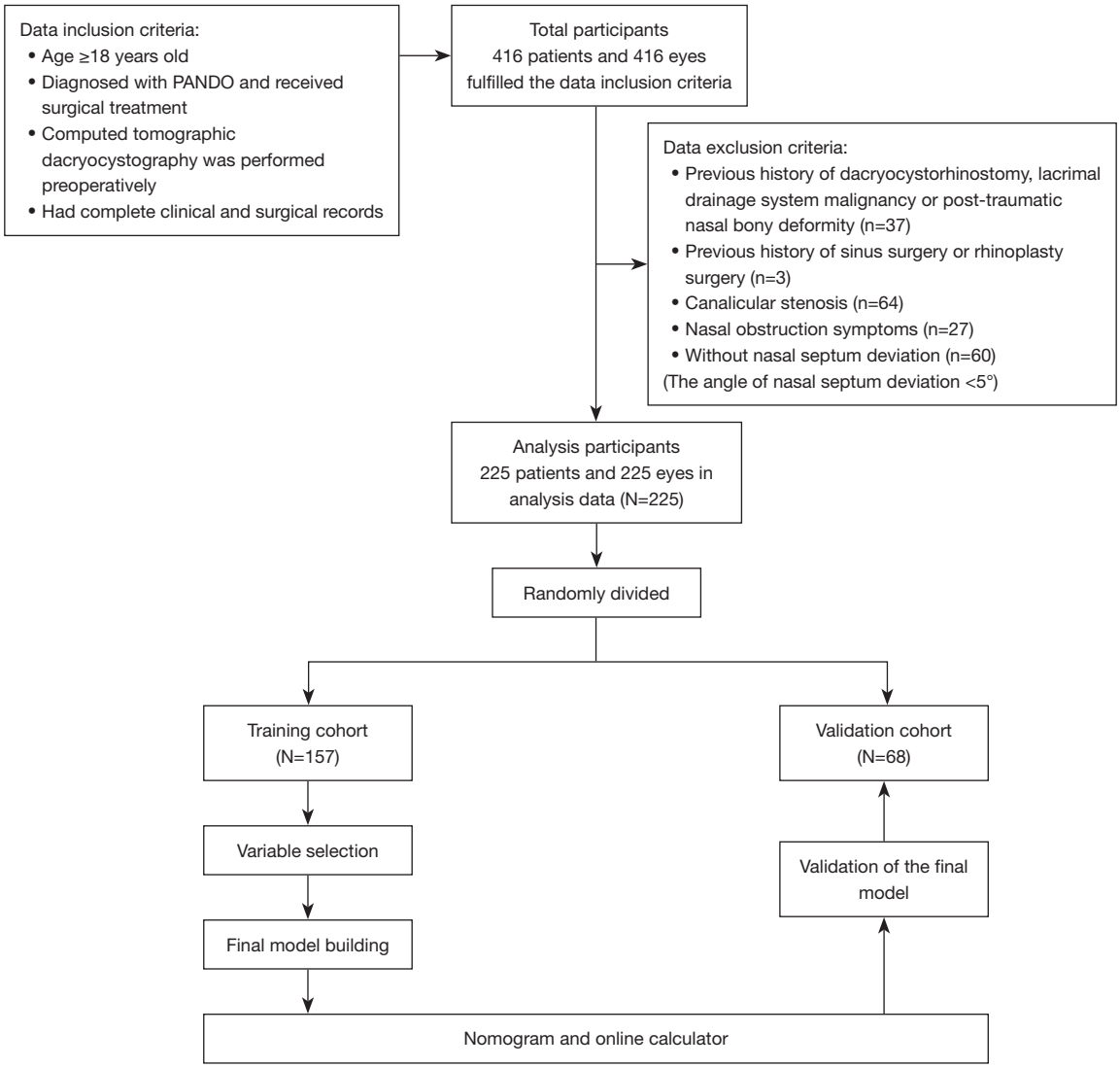

Figure 1 Flowchart of participant inclusion. PANDO, primary acquired nasolacrimal duct obstruction.

Ophthalmic Center were retrospectively collected.

Adult patients diagnosed with PANDO who had undergone surgery and for whom CT-DCG imaging and complete medical records were available were included in the study. Meanwhile, patients were excluded according to following criteria: a history of previous DCR, sinus, or rhinoplasty surgery; lacrimal drainage system malignancy; posttraumatic nasal bony deformity; nasal obstruction symptoms; or canalicular stenosis. Those who met the inclusion criteria but did not meet the exclusion criteria were enrolled in the study and were randomly divided into training and internal validation cohorts at a ratio of 7:3, respectively. A training cohort is a set of examples for learning that is to fit the parameters of the classifier, whereas a validation cohort is a set of samples used to provide an unbiased evaluation of a model fit on the training dataset while the model hyperparameters are tuned. The training cohort was used to select influential variables and generate a prediction model, while the internal validation cohort was used to test the prediction model (*Figure 1*).

CT-DCG image acquisition

Following verification of the patient's lack of iodized oil or contrast allergy history, a CT-DCG procedure was conducted by administering iodized oil contrast into the

lacrimal sac through the lacrimal puncta and canaliculus. With the patient supine, local anesthesia of the conjunctiva was performed with 0.5% proparacaine hydrochloride. Catheterization of the upper canaliculus of the affected eye was performed with a 27-guage lacrimal cannula (outer diameter =0.4 mm, inner diameter =0.15 mm; Inami, Tokyo, Japan) that was attached to a 2-mL syringe. A slow injection of 0.5 to 1.0 mL of an iodinated contrast medium (iodinated oil injection, 10 mL; Yantai Luyin Pharmaceutical Co., Ltd., Yantai Luyin, Yantai, China) was completed as a series of radiographs was acquired.

Without any type of nasal decongestant, a 64-slice high-speed scanner (SOMATOM Definition AS; Siemens Healthineers, Erlangen, Germany) was used for image acquisition in all participants. Contiguous nonoverlapping sections of a cranio-orbital CT scan were achieved in helical mode with a slice thickness of 1.00 mm, 120 kV, and 200 mAs. Images were sent to a CT workstation (Siemens Healthineers) for assessment. Reformatted images in the sagittal and coronal planes were constituted in addition to the axial plane with the same resolution characteristics. Images were evaluated with both bone and soft-tissue algorithms.

Image analysis

Image assessment was performed by a single investigator using the picture archiving and communication system (PACS). The following measurements were performed on 1.00-mm coronal reformations that were rendered in a bone algorithm and viewed at a window level and width of 800 and 2,000 Hounsfield units (HU), respectively: (I) vertical size of the lacrimal sac, (II) NSD angle, (III) NSD height, (IV) NSD direction, (V) NSD location, (VI) middle nasal passage width (MNPW) at the surgical side, (VII) minimal cross-sectional area of the nasal cavity airway (CANCA) in the surgical region, (VIII) NSD type, and (IX) variations in nasal anatomy.

The vertical diameter of the lacrimal sac in the coronal plane was measured by identifying the level at which the largest lacrimal sac visualization occurred and was subsequently categorized into two groups: small (<5 mm) or not small (≥5 mm) (22). Based on the image on which the NSD was most severe, two reference coordinates of the most anterior maxillary crest and crista galli were marked, and a vertical reference line between these two points was used for each measurement. The angle of NSD was measured on coronal CT images as the angle between the most deviated point of the septum and the midline (*Figure 2A*) (18). The vertical distance from the apex to the floor of the nasal cavity was measured parallel to the midline (NSD height), and the direction and most deviated location of septal deviation was recorded (*Figure 2A*). The nasal septum can be classified into different segments of deviation based on the location of the most prominent point of the deviation, including the anterior, middle, and posterior segments, in a manner similar to the CT grading system for NSD outlined by Ardeshirpour *et al.* (23). We evaluated the impact of the most deviated point of the septum on the En-DCR procedure, delineating between the surgical and nonsurgical regions. The surgical region was defined as that extending from the external nostril to the level of the head of the middle turbinate. The MNPW at the surgical side was measured in the coronal plane by selecting the level with the largest lacrimal sac visualization, and it was defined as the distance between the frontal processes of maxilla and the nasal septum on the operated side (*Figure 2B*). Minimal cross-sectional intranasal areas of the surgical passage were identified in the surgical region and then outlined and calculated (*Figure 2C*) (18). The modified Guyuron classification of septal deformities, which is convenient to use in daily practice, was used to classify septal deviation (24). Type A deformities included Guyuron classes I and VI (septal tilt and localized spicule, respectively), type B deformities included Guyuron classes II and III (C-shaped anteroposterior and cephalocaudal septal deviations, respectively), and type C deformities included Guyuron classes IV and V (S-shaped anteroposterior and cephalocaudal septal deviations, respectively) (*Figure 2D-2F*). Finally, other pathologies of the nasal cavity (turbinate hypertrophy, concha bullosa, nasal polyp, etc.), if present, were recorded as variations in nasal anatomy (*Figure 2G-2I*).

Surgical method

The En-DCR was conducted as previously reported (25), with all procedures being performed under general anesthesia by the same skilled surgeon (X.L.). In cases where patients exhibited a narrow En-DCR surgical corridor due to NSD, a restricted nasal septoplasty was performed, as indicated in a prior study (26). In patients with severe lacrimal sac mucosal injury (such as traumatic lacrimal sac rupture, severe lacrimal sac mucosal scarring due to recurrence after lacrimal duct recanalisation, or intraoperative presentation of dacryoliths) and in patients with combined obstruction or stenosis of the canaliculi or

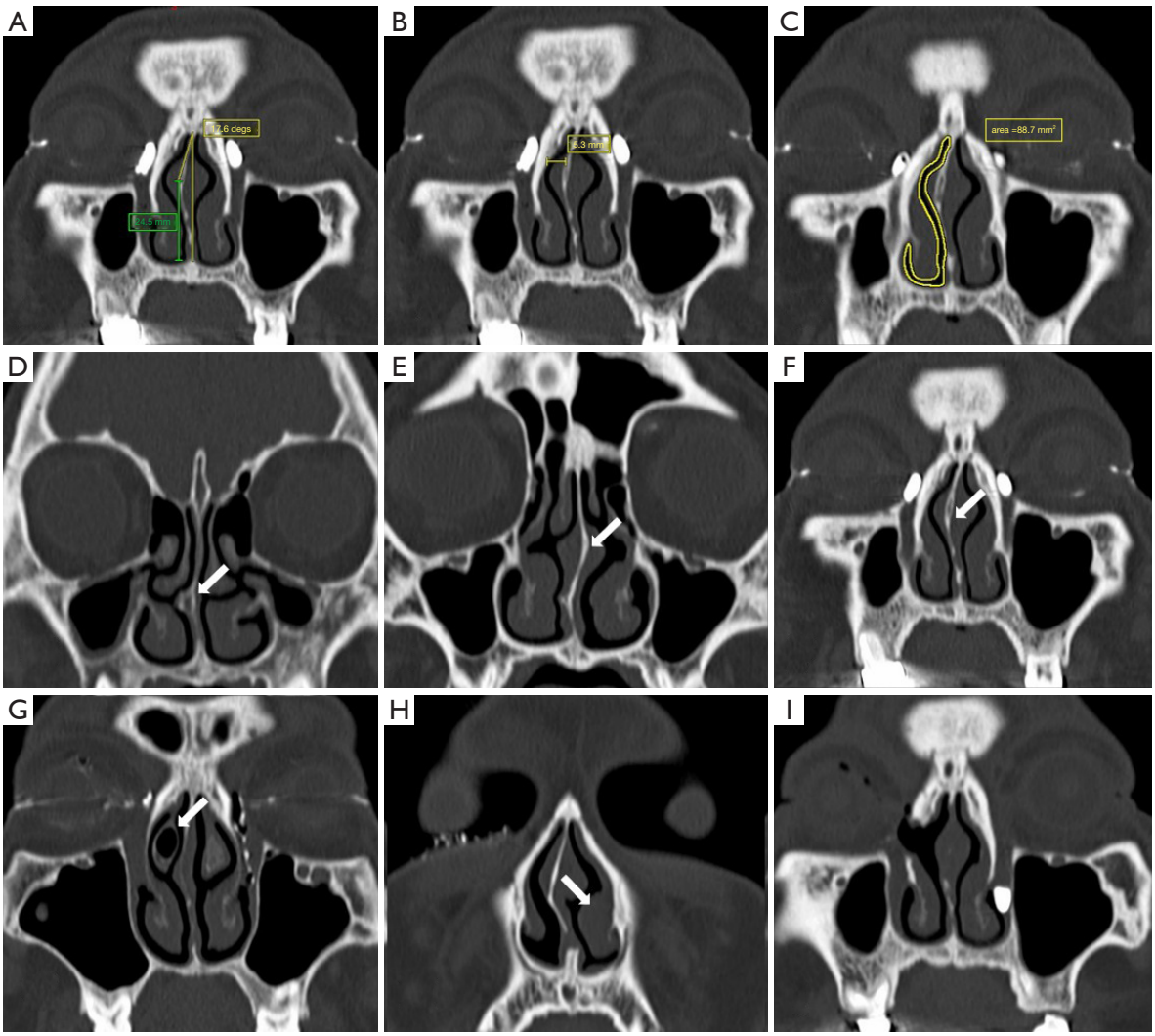

Figure 2 Anatomic characteristics measured and evaluated by computed tomography. (A) The angle of NSD was measured on coronal CT images as the angle between the most deviated point of the septum and the midline. The height of NSD was the vertical distance from the apex of NSD to the floor of the nasal cavity and was measured parallel to the midline (green line). (B) The MNPW on the surgical side was measured in the coronal plane by selecting the level with the largest lacrimal sac visualization and was defined as the distance between the frontal processes of maxilla and the nasal septum on the operated side. (C) The minimal cross-sectional intranasal areas of the surgical passage were identified at the surgical region and then outlined and calculated. (D-H) The modified Guyuron classification of septal deformities: (D) septal tilt and localized spicule, (E) S-shaped anteroposterior and cephalocaudal septal deviations, (F) C-shaped anteroposterior and cephalocaudal septal deviations, (G) concha bullosa on the surgical side, and (H) inferior turbinate hypertrophy on the nonsurgical side (white arrows). (I,F) Images from the same patient with bilateral PANDO; the right eye was the first to be treated with En-DCR in combination with septoplasty. (I) Image obtained during the preoperative examination of this patient's left eye, which indicated a patent anastomosis and a well-corrected septum in the right eye after surgery. NSD, basal septal deviation; CT, computed tomography; MNPW, middle nasal passage width; PANDO, primary acquired nasolacrimal duct obstruction; En-DCR, endonasal endoscopic dacryocystorhinostomy.

common canaliculi, a silicone tube was inserted from the upper and lower punctum to the nasolacrimal duct and grasped with Blakesley forceps. The ends of the tubing were then tied and trimmed within the nasal cavity to form a continuous loop around the canaliculi.

Follow-up

Patients underwent assessments for symptoms, tear duct irrigation, and nasal endoscopy at 1, 3, and 6 months postoperatively. If present, the silicone tube was typically removed between 4 to 6 weeks after surgery. All patients underwent a follow-up examination at a minimum of 6 months after surgery for evaluation of symptoms and complications. The assessment included monitoring for common postoperative complications such as nasal bleeding, nasal congestion, stent prolapse, sinusitis, emphysema, and headaches. The success of the surgical intervention was determined based on the relief of symptoms and the patency of tear duct irrigation.

Statistical analysis

Excel 365 (Microsoft Corp., Redmond, WA, USA) was used for data collection and collation. The "glmnet" package in R 4.3.2 (The R Foundation of Statistical Computing, Vienna, Austria) was used to process data. All continuous variables, except for symptom duration, conformed to a normal distribution and were presented as the mean ± standard deviation; symptom duration was expressed as the median and interquartile range. Categorical variables were expressed as the frequency and percentage. The comparability of the two sets was further assessed through *t*-tests, χ^2 tests, or the Mann-Whitney test, as appropriate. The training set was applied for baseline variable selection and nomogram development. To minimize the potential collinearity of variables and overfitting of the model, least absolute shrinkage and selection operator (LASSO) regression and 10-fold cross-validation were applied for predictor selection. Subsequently, a multivariate logistic regression model was constructed to further select the most significant variables (P<0.05). The nomogram model was then established according to multivariate logistic regression, and the receiver operating characteristic (ROC) curve and area under the curve (AUC) were used to verify the prediction efficacy of the model. The bootstrap resampling method and calibration curve were used to evaluate the consistency of the model, and the net benefit of patients was evaluated with clinical decision curve analysis (DCA). The fitness of the final prediction model was assessed using the Akaike information criterion (AIC) (a lower AIC indicates better model fit), the Cox-Snell R-squared statistic, and the Nagelkerke R-squared statistic. Concordance statistics, calibration, and DCA were applied to validate the internal stability of the model. The significance level was set at 0.05, and all tests were two-sided.

Results

Characteristics of the participants

After screening 416 patients in our hospital's patient registry, 225 patients (mean age: 56 years, SD 12 years; females: n=191, 84.9%) were included in this study, 157 of whom were enrolled in the training cohort and 68 in the validation dataset. There were no significant differences between the datasets in terms of demographic or CT measurement parameters. All of the P values for these patients were greater than 0.05 and are presented in *Table 1*. All 225 patients underwent unilateral En-DCR, and 53 of them underwent concurrent septoplasty (53/225, 23.6%). By reviewing postoperative visit records and conducting telephone follow-up 6 months after surgery, we found that the functional success rates were similar between the two groups. Postoperative complications occurred in 7 patients (13.2%, 7/53) who underwent En-DCR with septoplasty and 16 patients (9.3%, 16/172) who underwent En-DCR alone. There was one case of septal perforation and six cases of hemorrhage in the En-DCR plus septoplasty group. The complications in the En-DCR-alone group included hemorrhage (*Table 2*), which occurred directly after surgery and was treated with nasal packing. The baseline characteristics of each dataset are presented in Table S1 and include data on the surgical decision to combine septoplasty and En-DCR or to use En-DCR alone.

Comparison of CT measurement parameters and radiological features

The CT measurement parameters and the radiological features of the patients with PANDO and NSD who had undergone En-DCR alone and those who had undergone En-DCR with septoplasty are summarized in *Table 3*. According to the univariate analysis, the CT measurement parameters and radiological features that were significantly

Table 1 Characteristics of the training and validation sets of patients with PANDO with NSD

Characteristic	Patients with PANDO and NSD			P value
	Overall (N=225)	Training cohort (N=157)	Internal test cohort (N=68)	
Gender, n (%)				0.131
Female	191 (84.9)	137 (87.3)	54 (79.4)	
Male	34 (15.1)	20 (12.7)	14 (20.6)	
Age (years), mean ± SD	56±12	57±12	56±12	0.711
Surgery eye, n (%)				0.443
Right eye	117 (52.0)	79 (50.3)	38 (55.9)	
Left eye	108 (48.0)	78 (49.7)	30 (44.1)	
Symptom duration (months), median [IQR]	24 [12, 48]	24 [11, 60]	20 [12, 48]	0.682
Eye surgery and medication history, n (%)				0.740
Absent	196 (87.1)	136 (86.6)	60 (88.2)	
Lacrimal duct recanalization	29 (12.9)	21 (13.4)	8 (11.8)	
Systemic conditions[†], n (%)				0.635
Absent	181 (80.4)	125 (79.6)	56 (82.4)	
Present	44 (19.6)	32 (20.4)	12 (17.6)	
Vertical size of lacrimal sac (mm), n (%)				0.828
≥5	180 (80.0)	125 (79.6)	55 (80.9)	
<5	45 (20.0)	32 (20.4)	13 (19.1)	
NSD type, n (%)				0.583
C-shaped deviation	91 (40.4)	67 (42.7)	24 (35.3)	
Localized deviation	103 (45.8)	69 (43.9)	34 (50.0)	
S-shaped deviation	31 (13.8)	21 (13.4)	10 (14.7)	
NSD angle (degree), mean ± SD	10.6±4.1	10.5±4.0	11.1±4.2	0.337
NSD height (mm), mean ± SD	17.3±4.7	17.4±4.8	17.1±4.5	0.726
NSD location, n (%)				0.239
Non-surgical approach area	109 (48.4)	72 (45.9)	37 (54.4)	
Surgical approach area	116 (51.6)	85 (54.1)	31 (45.6)	
Minimal CANCA at surgical region (mm^2), mean ± SD	154±26	153±26	156±26	0.327
MNPW at surgical side (mm), mean ± SD	9.1±2.1	9.1±2.1	9.2±2.1	0.677
NSD direction, n (%)				0.196
Opposite side	114 (50.7)	84 (53.5)	30 (44.1)	
Surgical side	111 (49.3)	73 (46.5)	38 (55.9)	
Variations in nasal anatomy[‡], n (%)				0.390
Absent	153 (68.0)	104 (66.2)	49 (72.1)	
Present	72 (32.0)	53 (33.8)	19 (27.9)	

[†], the systemic conditions exhibited by the participants encompassed hypertension, diabetes, coronary heart disease, and rheumatic diseases; [‡], among the 225 patients, 72 individuals (72/225, 32.0%) exhibited nasal abnormalities. Specifically, inferior turbinate hypertrophy on the surgical side was observed in 52 cases (52/225, 23.1%), concha bullosa on the surgical side in 17 cases (17/225, 7.6%), and nasal polyps on the surgical side in 3 cases (3/225, 1.3%). PANDO, primary acquired nasolacrimal duct obstruction; NSD, nasal septal deviation; SD, standard deviation; IQR, interquartile range; CANCA, cross-sectional area of the nasal cavity airway at surgical region; MNPW, middle nasal passage width.

Table 2 Surgical outcomes and complications of two groups

Variable	Treatment decision		P value†
	En-DCR with septoplasty (N=53)	En-DCR without septoplasty (N=172)	
Postoperative complications, n (%)			0.230
Hemorrhage	6 (11.3)	16 (9.3)	
Septal perforation	1 (1.9)	0 (0.0)	
Functional success, n (%)	45 (84.9)	152 (88.4)	0.504

†, Fisher exact test or Pearson chi-squared test. En-DCR, endonasal endoscopic dacryocystorhinostomy.

Table 3 Comparison of CT measurement parameters and the radiological features.

Characteristic	Overall (N=225)	Treatment decision		P value†
		En-DCR without septoplasty (N=172)	En-DCR with septoplasty (N=53)	
Surgery eye, n (%)				0.043*
Right eye	117 (52.0)	83 (48.3)	34 (64.2)	
Left eye	108 (48.0)	89 (51.7)	19 (35.9)	
Vertical size of lacrimal sac (mm), n (%)				0.034*
≥5	180 (80.0)	143 (83.1)	37 (69.8)	
<5	45 (20.0)	29 (16.9)	16 (30.2)	
NSD type, n (%)				0.129
C-shaped deviation	91 (40.4)	64 (37.2)	27 (50.9)	
Localized deviation	103 (45.8)	85 (49.4)	18 (34.0)	
S-shaped deviation	31 (13.8)	23 (13.4)	8 (15.1)	
NSD angle (degree), mean ± SD	10.6±4.1	9.5±3.5	14.2±3.8	<0.001*
NSD height (mm), mean ± SD	17.3±4.7	17.2±5.0	17.6±3.7	0.532
Minimal CANCA at surgical region (mm^2), mean ± SD	154±26	158±25	141±24	<0.001*
MNPW at surgical side (mm), mean ± SD	9.1±2.1	9.7±1.9	7.4±1.8	<0.001*
NSD location, n (%)				0.016*
Nonsurgical approach area	109 (48.4)	91 (53.0)	18 (34.0)	
Surgical approach area	116 (51.6)	81 (47.1)	35 (66.0)	
NSD direction, n (%)				0.014*
Opposite side	114 (50.7)	95 (55.2)	19 (35.9)	
Surgical side	111 (49.3)	77 (44.8)	34 (64.2)	
Variations in nasal anatomy, n (%)				0.090
Absent	153 (68.0)	122 (70.9)	31 (58.5)	
Present	72 (32.0)	50 (29.1)	22 (41.5)	

†, Pearson chi-squared test; Welch two-sample *t*-test. *, significant P value 0.05. CT, computed tomography; En-DCR, endonasal endoscopic dacryocystorhinostomy; NSD, nasal septal deviation; CANCA, cross-sectional area of the nasal cavity airway at surgical region; MNPW, middle nasal passage width.

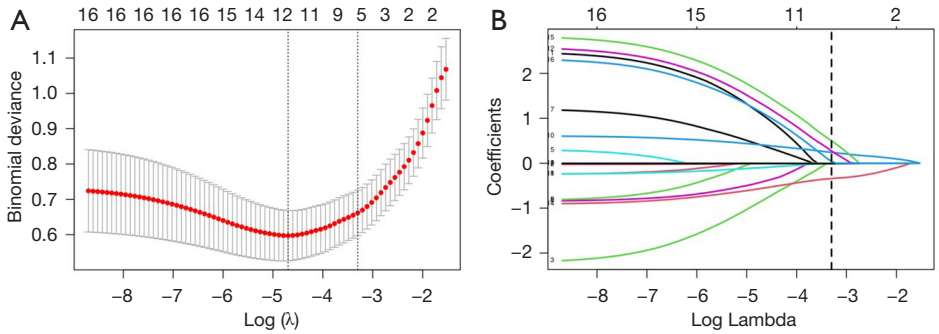

Figure 3 Feature selection with LASSO Cox regression. (A) Tuning parameter (λ) selection cross-validation error curve. (B) Plot of the LASSO coefficient profiles. LASSO, least absolute shrinkage and selection operator.

Table 4 Risk factors selected by the LASSO logistic regression model

Risk factor	Coefficient
NSD angle	0.2416
NSD location	0.2734
Minimal CANCA at surgical region	−0.0085
MNPW at surgical side	−0.3414
NSD direction	0.4999
Variations in nasal anatomy	0.0407

LASSO, least absolute shrinkage and selection operator; NSD, nasal septal deviation; CANCA, cross-sectional area of the nasal cavity airway at surgical region; MNPW, middle nasal passage width.

different between the two groups included vertical size of lacrimal sac, NSD angle, minimal CANCA in the surgical region, MNPW at the surgical side, NSD location, and NSD direction (P<0.05). Both the percentages of right eye surgeries and small vertical size of lacrimal sac in patients treated with En-DCR with septoplasty were higher than those treated with En-DCR alone (P<0.05). In patients treated with En-DCR alone, the mean values of NSD angle, minimal CANCA in the surgical region, and MNPW at the surgical side were 9.5°±3.5°, 158±25 mm^2, and 9.7±1.9 mm, respectively; meanwhile, for those treated with En-DCR and septoplasty, these values were 14.2°±3.8°, 141±24 mm^2, and 7.4±1.8 mm, respectively, representing statistically significant differences between the groups (all P values <0.05). The percentage of the most deviated location of NSD in the surgical region and NSD to the operative side were higher in patients who undergone En-DCR with septoplasty (P<0.05). However, the other CT measurement parameters and the radiological features were not significantly different between the groups (P >0.05) (*Table 3*). Among the 225 patients, 72 (32.0%) exhibited nasal abnormalities. Specifically, inferior turbinate hypertrophy on the surgical side was observed in 52 cases (52/225, 23.1%), concha bullosa on the surgical side in 17 cases (17/225, 7.6%), and nasal polyps on the surgical side in 3 cases (3/225, 1.3%). The differences in nasal anatomy between the two groups were not statistically significant (P>0.05).

Variable selection and prediction model construction

Fifteen baseline variables (*Table 1*) were included in the LASSO regression for the training cohort. A cross-validated error plot of the LASSO regression model is shown in *Figure 3A*, and a coefficient profile is plotted in *Figure 3B*. As depicted in *Figure 3A*, the most regularized and parsimonious model with cross-validated error within one standard error of the minimum, identified six variables (*Table 4*) as candidate indicators for the surgical decision of concomitant endoscopic septoplasty. To further screen the most valuable predictors, the indicators were incorporated into a multivariate logistic regression model, and four indicators with P<0.05 were retained as independent predictors (*Figure 4*). In terms of the Bayesian information criterion, the model based on the four predictors performed best. The final model had an AIC of 76.71, a concordance statistic of 0.913, a Cox-Snell R-squared value of 0.399, and a Nagelkerke R-squared value of 0.610. No collinear relationship was detected (variance inflation factor <5.0). Finally, a nomogram was generated for predicting the probability of concomitant endoscopic septoplasty during

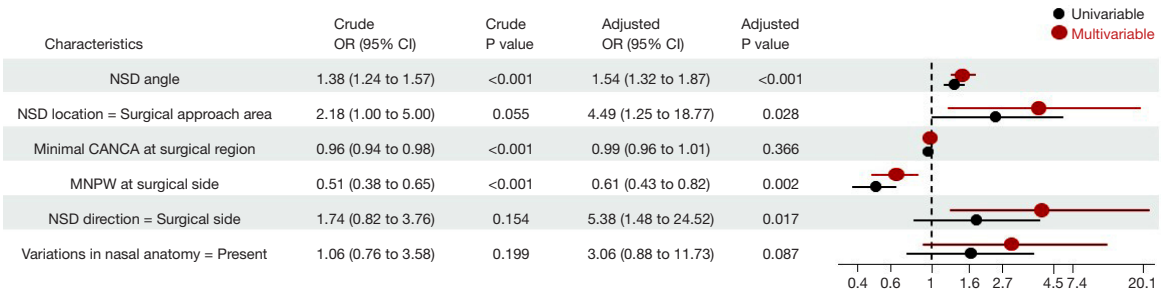

Figure 4 Influencing factors of concomitant endoscopic septoplasty surgical decision in patients with PANDO with NSD in the univariate and multivariable analyses. OR, odds ratio; CI, confidence interval; NSD, nasal septal deviation; CANCA, cross-sectional area of the nasal cavity airway at surgical region; MNPW, middle nasal passage width; PANDO, primary acquired nasolacrimal duct obstruction.

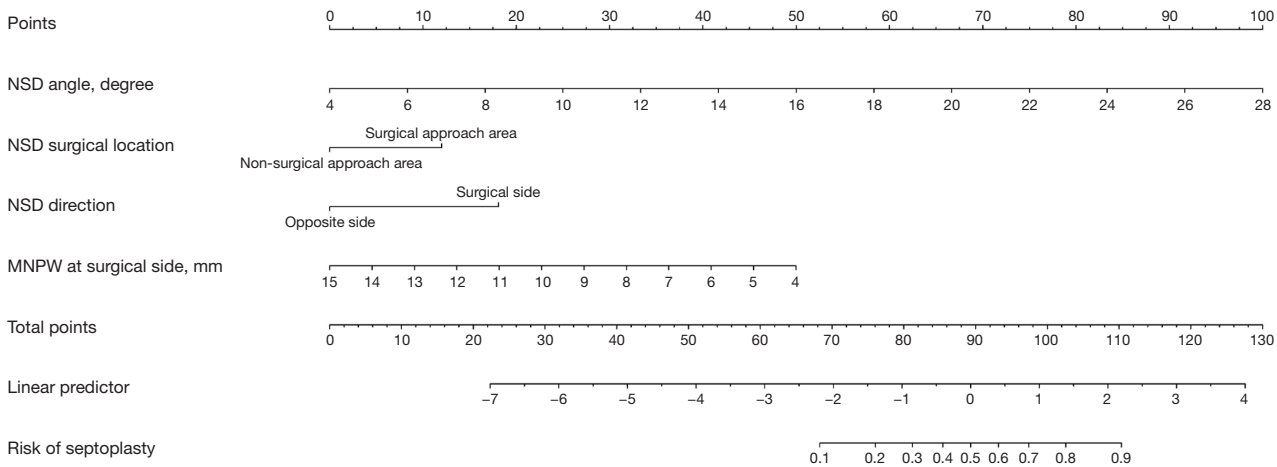

Figure 5 The nomogram for estimating the risk of concomitant endoscopic septoplasty during En-DCR in patients with PANDO. NSD, nasal septal deviation; MNPW, middle nasal passage width; En-DCR, endonasal endoscopic dacryocystorhinostomy; PANDO, primary acquired nasolacrimal duct obstruction.

En-DCR with the four predictors, which included NSD angle degrees [odds ratio (OR) 1.54; 95% confidence interval (CI): 1.32–1.87], NSD location (OR 4.49; 95% CI: 1.25–18.77), NSD direction (OR 5.38; 95% CI: 1.48–24.52), and MNPW at the surgical side (OR 0.61; 95% CI: 0.43–0.82) The nomogram is illustrated in *Figure 5* and Figure S1 and is also available online (https://zocdcrs.shinyapps.io/dynnomapp/).

Validation and performance of the nomogram

As shown in *Figure 6A,6B*, the AUCs of the model in the training cohort and internal validation cohort were 0.913 and 0.909, respectively, indicating good predictive ability. The internal validation and calibration of the nomogram were performed using 1,000 bootstrap analyses. The calibration curve was used to evaluate the predictive power (*Figure 7A,7B*). The predictive model and the validation set showed the optimal predictive degree of the fitting. DCA was then applied to evaluate the net benefit for patients in clinical practice. The results suggested that the nomogram has good clinical application value (*Figure 8A,8B*).

Discussion

This study identified four risk factors for concomitant septoplasty during En-DCR in patients with PANDO and NSD: NSD angle, NSD location, NSD direction, and MNPW at the surgical side. All four predictors are available and easily obtained from preoperative examinations through consistent and well-accepted measurement procedures. To the best of our knowledge, this is the first study to identify

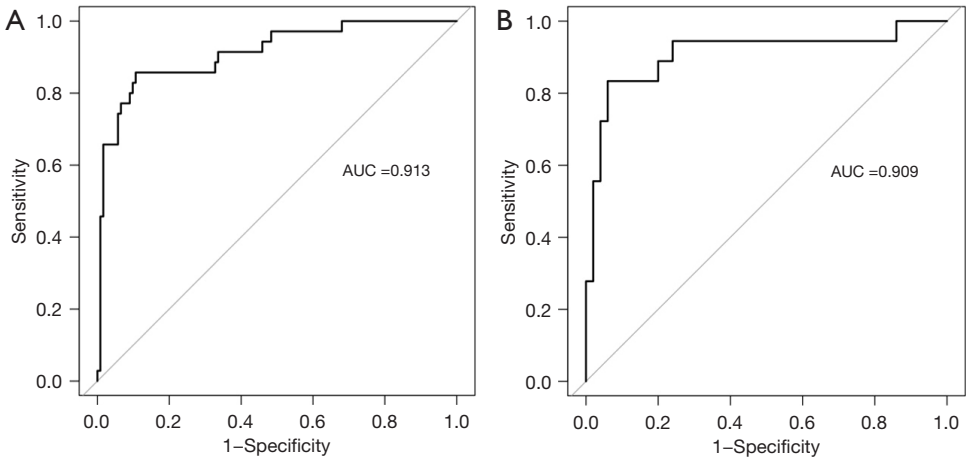

Figure 6 ROC of the nomogram for (A) the training cohort and (B) the internal validation cohort. ROC, receiver operating characteristic; AUC, area under the curve.

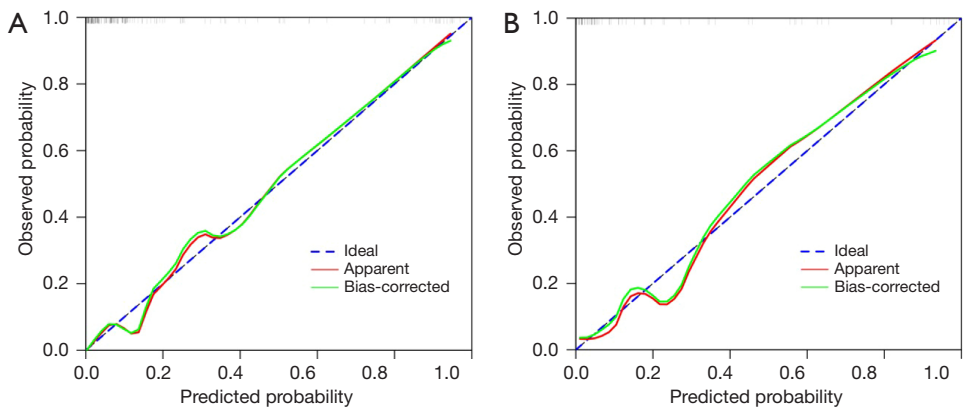

Figure 7 The calibration plots of (A) the training cohort and (B) the internal validation cohort. The x-axis represents the nomogram-predicted probability, and the y-axis represents the actual probability of surgical risks of concomitant endoscopic septoplasty during En-DCR. A perfect prediction would correspond to the 45° blue dashed line. The red solid line represents the entire cohort in the training cohort (n=157) and internal validation cohort (n=68), respectively. The green solid line is the bias-corrected bootstrapping (B=1,000 repetitions), indicating observed nomogram performance. En-DCR, endonasal endoscopic dacryocystorhinostomy.

CT-based risk factors for concomitant septoplasty during En-DCR in patients with PANDO with NSD. In addition, this study outlined the factors in predicting the risk of concomitant septoplasty during En-DCR via a nomogram and confirmed through internal validation that the model had a high predictive ability. The accuracy in the training cohort and testing cohort was 0.913 and 0.909, respectively.

Limited nasal septoplasty can be performed in the same operating session before DCR, allowing for better surgical exposure (7,26,27). The reported rate of concomitant En-DCR and septoplasty for NSD is considerable, and ranges from 11.9% to 57% (11,12,27). In this study, the rate of concomitant En-DCR and septoplasty in patients with PANDO and NSD was 23.6%. Some studies have reported that concomitant endoscopic septoplasty during En-DCR does not affect surgical prognosis but does reduce complications and that septoplasty should be considered when indicated to improve surgical access (11,12). Consistent with previous studies, our results suggest that concomitant endoscopic septoplasty during En-DCR does not affect surgical prognosis. The functional success rate was 88.4% in patients undergoing unilateral EN-DCR

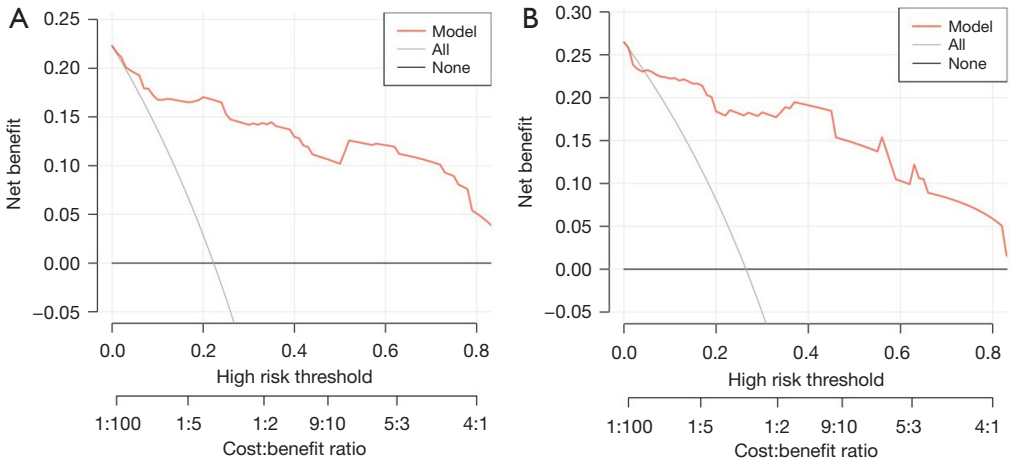

Figure 8 Nomogram decision curves for (A) the training cohort and (B) the internal validation cohort. The y-axis shows the net benefit. The x-axis shows the corresponding high-risk threshold. The gray line represents the assumption that all patients with PANDO and NSD underwent concomitant endoscopic septoplasty during En-DCR. The black line represents the assumption that all patients with PANDO and NSD underwent En-DCR alone. The decision curve shows that if the threshold probability is over 5%, using the nomogram to predict surgical risk of concomitant endoscopic septoplasty during En-DCR adds more benefit than does either the all-treated scheme or the none-treated scheme. PANDO, primary acquired nasolacrimal duct obstruction; NSD, nasal septal deviation; En-DCR, endonasal endoscopic dacryocystorhinostomy.

and 84.9% in those undergoing En-DCR combined with nasal septoplasty, and these rates were not statistically different. There is currently a lack of criteria for the preoperative selection of concomitant septoplasty during En-DCR in part because there has been no standard and objective method for evaluating NSD in patients with PANDO. The use of low-dose helical CT-DCG with the reconstruction of coronal and sagittal planes is considered an optimal imaging modality, as it provides minimal radiation exposure for the identification of nasolacrimal duct obstruction (28). The integration of CT with DCG enables the precise visualization of lacrimal duct blockages or stenoses, providing critically useful assessment of patients with suspected lacrimal sac diverticula or lacrimal drainage tumors. This combined imaging modality provides reliable information for informing the selection of appropriate surgical interventions (16,17). Additionally, a CT scan is a recommended objective assessment method for determining the severity of NSD, especially for middle and posterior deviations of the septum (29).

NSD can narrow the middle meatus by pushing the concha laterally and can be classified based on its morphology, angle, and location. However, there are no universally accepted classifications for septal deviation (24,30,31). In our study, the modified Guyuron classification of septal deformities was used to classify the septal deviation, as it is easier to use in daily practice. In order to evaluate the size of nasal surgical field and to NSD, several objective parameters on CT scans were used in this study. A coronal CT scan image showing the area of surgical access was performed for the evaluation of the direction and degree of septal deviation. The average NSD angle was found to be 9.5°±3.5°, which is lower than the 13°±3.4° reported by Kapusuz Gencer *et al.* (32). This difference may be attributed to the absence of nasal obstruction symptoms in the patients included in our study, indicating a lower severity of NSD in this cohort. The degree of NSD angle was a significant risk factor for concomitant septoplasty during En-DCR. A greater NSD angle may increase the likelihood of requiring septoplasty during En-DCR surgery, as it limits the surgical field. The type of NSD classified according the Guyuron method was not relevant to the surgical decision of concomitant septoplasty during En-DCR, possibly because this classification method is based on the morphology of the deviated septum, and the morphology of the deviated septum has little effect on the size of the nasal cavity on the surgical side. The location of NSD was found to be a significant risk factor for surgical decision. As the operculum of the middle turbinate (OMT) and maxillary line have been recognized as important

anatomical criteria for locating the lacrimal sac and the surgical area (33), we defined the surgical access area as the plane from the external nostril to the OMT. Maximal septal deviation within the surgical area has a greater impact on the surgical access space for En-DCR than does a deviation outside the surgical area, such as posterior septal deviation.

Interestingly, we found that surgery on the right eye and a small vertical size of the lacrimal sac were more common in the patients treated with En-DCR and septoplasty than in those treated with En-DCR alone. In general, the operator stands on the right side of the patient during the En-DCR procedure, making it easier to incise and expose the left side of the lacrimal sac as compared to the right side. In this study, the vertical size of the lacrimal sac was classified using a cutoff of 5 mm, as reported by Lee *et al.* (22). In small lacrimal sacs, the intraoperative stoma position must be higher to improve the prognosis. The higher the stoma position is, the less space available for the surgical procedure and the greater the influence of NSD on the surgical procedure. Although the operative eye and vertical size of the lacrimal sac may influence the difficulty of En-DCR, they were not the important factors in the surgical decision of concomitant septoplasty during En-DCR in our study. The minimal cross-sectional area of the nasal cavity airway in the surgical region was a direct factor influencing the decision of concomitant septoplasty during En-DCR, but hypertrophy of the nasal mucosa has a significant effect on the minimum cross-sectional area of the nasal cavity, which increases after the use of decongestants. In addition, our study measured the minimum cross-sectional area of the nasal airway at the surgical region, which includes part of the nonsurgical area, and thus this measure cannot accurately reflect the size of the surgical field. The most common variation of nasal anatomy in this study was inferior turbinate hypertrophy, whose effect on the size of the surgical field can be minimized by the use of decongestants. Therefore, inferior turbinate hypertrophy was not included in our prediction model. The width of the midline nasal passage on the surgical side directly reflects the size of the operating room and was the main factor in the decision to perform concomitant septoplasty.

Preoperative CT imaging evaluation could serve as a reference to discern septal deviation requiring correction during the surgical planning for PANDO. Based on CT features, this study developed a prediction model of the surgical decision of concomitant septoplasty during En-DCR using LASSO. The model showed high predictive ability through internal validation and has good clinical application value.

Our study had several limitations that need to be acknowledged. We employed a retrospective design, which might have led to bias in the data. As the observational cohorts only included patients referred to our tertiary care center and as the experience of the surgeon can influence the decision of concomitant septoplasty during En-DCR, the risk of concomitant septoplasty during En-DCR and the statistical weight of the proposed predictors might have been underestimated. Moreover, the validation of this nomogram was only based on an internal validation cohort, and thus further validation in a prospective validation set and in multiple centers is necessary.

Conclusions

In this study, the independent factors for concomitant septoplasty during En-DCR in patients with PANDO and NSD included NSD angle, NSD location, NSD direction, and MNPW at the surgical side. Based on these CT characteristics, the nomogram model of the need of concomitant septoplasty during En-DCR established by LASSO regression showed a good predictive performance. The model quantified the preoperative judgement of surgeons regarding the need for concomitant septoplasty during En-DCR. This model has the potential to aid surgeons in assessing the necessity of concomitant septoplasty during En-DCR, thereby enabling a personalized approach to perioperative care and ultimately enhancing patient outcomes.

Acknowledgments

Funding: This study was supported by Guangdong Science and Technology Programme for Social Development (No. 3030901005237 to X.L.).

Footnote

Reporting Checklist: The authors have completed the TRIPOD reporting checklist. Available at https://qims.amegroups.com/article/view/10.21037/qims-24-726/rc

Conflicts of Interest: All authors have completed the ICMJE uniform disclosure form (available at https://qims.amegroups.com/article/view/10.21037/qims-24-726/coif). The authors have no conflicts of interest to declare.

Ethical Statement: The authors are accountable for all aspects

of the work in ensuring that questions related to the accuracy or integrity of any part of the work are appropriately investigated and resolved. This study was approved by the Institutional Review Board of the Zhongshan Ophthalmic Center, Sun Yat-sen University, China (No. 2021KYPJ100) and adhered to the tenets of the Declaration of Helsinki (as revised in 2013). The institutional review board waived the requirement for informed consent owing to the retrospective nature of the study.

References

1. Yigit O, Samancioglu M, Taskin U, Ceylan S, Eltutar K, Yener M. External and endoscopic dacryocystorhinostomy in chronic dacryocystitis: comparison of results. Eur Arch Otorhinolaryngol 2007;264:879-85.
2. Ali MJ. Etiopathogenesis of primary acquired nasolacrimal duct obstruction (PANDO). Prog Retin Eye Res 2023;96:101193.
3. Jawad A, Kausar A, Iftikhar S, Akhtar N, Rabbani Z. Results of endoscopic endonasal dacryocystorhinostomy: A prospective cohort study. J Pak Med Assoc 2021;71:1420-3.
4. Fayet B, Racy E, Assouline M. Complications of standardized endonasal dacryocystorhinostomy with unciformectomy. Ophthalmology 2004;111:837-45.
5. Evereklioglu C, Sener H, Polat OA, Sonmez HK, Gunay Sener AB, Horozoglu F. Success rate of external, endonasal, and transcanalicular laser DCR with or without silicone stent intubation for NLD obstruction: a network meta-analysis of randomized controlled trials. Graefes Arch Clin Exp Ophthalmol 2023;261:3369-84.
6. Yim M, Wormald PJ, Doucet M, Gill A, Kingdom T, Orlandi R, Crum A, Marx D, Alt J. Adjunctive techniques to dacryocystorhinostomy: an evidence-based review with recommendations. Int Forum Allergy Rhinol 2021;11:885-93.
7. Kim SW, Yeo SC, Joo YH, Cho HJ, Seo SW, Jeon SY. Limited endoscopic high septoplasty prior to endonasal dacryocystorhinostomy: Our experience of nine cases. Clin Otolaryngol 2017;42:1363-6.
8. Reitzen SD, Chung W, Shah AR. Nasal septal deviation in the pediatric and adult populations. Ear Nose Throat J 2011;90:112-5.
9. Marcet MM, Kuk AK, Phelps PO. Evidence-based review of surgical practices in endoscopic endonasal dacryocystorhinostomy for primary acquired nasolacrimal duct obstruction and other new indications. Curr Opin Ophthalmol 2014;25:443-8.
10. Figueira E, Al Abbadi Z, Malhotra R, Wilcsek G, Selva D. Frequency of simultaneous nasal procedures in endoscopic dacryocystorhinostomy. Ophthalmic Plast Reconstr Surg 2014;30:40-3.
11. Koval T, Zloto O, Yakirevitch A, Ben Simon GJ, Ben-Shoshan J, Ben Artsi E, Weissman A, Priel A. No impact of nasal septoplasty on the outcome of endoscopic dacryocystorhinostomy. Eye (Lond) 2020;34:1454-8.
12. Zhang J, Ming S, Qing H, Han W, Li S. Prognosis of concurrent endoscopic dacryocystorhinostomy and nasal septoplasty for chronic dacryocystitis with moderate nasal septum deviation. Indian J Ophthalmol 2024;72:S435-40.
13. Martins de Sousa M, Rebelo J, Martins S, Silveira H, Órfão T, Pinto Moura C. Is Computed Tomography Necessary Before Septoplasty? Correlation With Physical Examination and Patient Complaints. Cureus 2023;15:e38558.
14. Wotman M, Kacker A. What are the indications for the use of computed tomography before septoplasty? Laryngoscope 2016;126:1268-70.
15. Sedaghat AR, Kieff DA, Bergmark RW, Cunnane ME, Busaba NY. Radiographic evaluation of nasal septal deviation from computed tomography correlates poorly with physical exam findings. Int Forum Allergy Rhinol 2015;5:258-62.
16. Choi SC, Lee S, Choi HS, Jang JW, Kim SJ, Lee JH. Preoperative Computed Tomography Findings for Patients with Nasolacrimal Duct Obstruction or Stenosis. Korean J Ophthalmol 2016;30:243-50.
17. Udhay P, Noronha OV, Mohan RE. Helical computed tomographic dacryocystography and its role in the diagnosis and management of lacrimal drainage system blocks and medial canthal masses. Indian J Ophthalmol 2008;56:31-7.
18. Rowan NR, Soler ZM, Mace JC, Camilon MP, Palmer C, Jones RH, Smith TL, Schlosser RJ. Lack of impact of radiologic septal measurements upon patient symptoms

and performance of septoplasty during endoscopic sinus surgery. Rhinology 2020;58:323-32.
19. Lepley TJ, Frusciante RP, Malik J, Farag A, Otto BA, Zhao K. Otolaryngologists' radiological assessment of nasal septum deviation symptomatology. Eur Arch Otorhinolaryngol 2023;280:235-40.
20. Janovic N, Janovic A, Milicic B, Djuric M. Is Computed Tomography Imaging of Deviated Nasal Septum Justified for Obstruction Confirmation? Ear Nose Throat J 2021;100:NP131-6.
21. Susaman N, Çetiner H. Is septoplasty required whenever anterior septal deviation is present? J Laryngol Otol 2023;137:404-7.
22. Lee MJ, Kim IH, Choi YJ, Kim N, Choung HK, Khwarg SI. Relationship between lacrimal sac size and duration of tearing in nasolacrimal duct obstruction. Can J Ophthalmol 2019;54:111-5.
23. Ardeshirpour F, McCarn KE, McKinney AM, Odland RM, Yueh B, Hilger PA. Computed tomography scan does not correlate with patient experience of nasal obstruction. Laryngoscope 2016;126:820-5.
24. Teixeira J, Certal V, Chang ET, Camacho M. Nasal Septal Deviations: A Systematic Review of Classification Systems. Plast Surg Int 2016;2016:7089123.
25. Chen R, Liu S, Jiang A, Wumaier A, Yang Y, Yu X, Meng Z, Mao Y, Liang X. A simple and efficient technique for suturing and knotting during endoscopic dacryocystorhinostomy. Int Ophthalmol 2023;43:63-71.
26. Cheng AC, Wong AC, Sze AM, Yuen HK. Limited nasal septoplasty by ophthalmologists during endonasal dacryocystorhinostomy: is it safe? Ophthalmic Plast Reconstr Surg 2009;25:293-5.
27. Goel R, Nagpal S, Kumar S, Kamal S, Dangda S, Bodh SA. Our experience with transcanalicular laser-assisted endoscopic dacryocystorhinostomy (TCLADCR) in patients of chronic dacryocystitis with deviated nasal septum. Int Ophthalmol 2015;35:811-7.
28. Reichel O, Gora F, Dittrich M, Kugler V. Low-dose helical CT-dacryocystography in nasolacrimal duct obstruction-a prospective study. HNO 2019;67:600-5.
29. Lee DC, Shin JH, Kim SW, Kim SW, Kim BG, Kang JM, Cho JH, Park YJ. Anatomical analysis of nasal obstruction: nasal cavity of patients complaining of stuffy nose. Laryngoscope 2013;123:1381-4.
30. Lin JK, Wheatley FC, Handwerker J, Harris NJ, Wong BJ. Analyzing nasal septal deviations to develop a new classification system: a computed tomography study using MATLAB and OsiriX. JAMA Facial Plast Surg 2014;16:183-7.
31. Buyukertan M, Keklikoglu N, Kokten G. A morphometric consideration of nasal septal deviations by people with paranasal complaints; a computed tomography study. Rhinology 2003;41:21-4.
32. Kapusuz Gencer Z, Ozkırış M, Okur A, Karaçavuş S, Saydam L. The effect of nasal septal deviation on maxillary sinus volumes and development of maxillary sinusitis. Eur Arch Otorhinolaryngol 2013;270:3069-73.
33. Woo KI, Maeng HS, Kim YD. Characteristics of intranasal structures for endonasal dacryocystorhinostomy in asians. Am J Ophthalmol 2011;152:491-498.e1.

Cite this article as: Wang K, Yu X, Chen R, Guo L, Li J, Meng Z, Hu Y, Nie S, Liang X. Development and validation of a nomogram for predicting the need for concomitant endoscopic septoplasty during endonasal endoscopic dacryocystorhinostomy. Quant Imaging Med Surg 2024;14(9):6493-6507. doi: 10.21037/qims-24-726

